



# Performance Analysis of an LCL Filter with Active Damping and Resonant Control for Grid-Connected Inverter

Társila de Jesus Santos<sup>1\*</sup>, Consuelo Cristina Gomes Silva<sup>2</sup>, Felipe Mendes de Vasconcellos<sup>3</sup>, Jairo Cavalcanti Amaral<sup>2</sup>, Calisto José da Silva Neto<sup>4</sup>, Henrique Cerqueira Lima Silva<sup>1</sup>, Luiz Henrique Santos Silva<sup>2</sup>

<sup>1</sup> Federal University of Reconcavo of Bahia (UFRB), Energy Engineering Student, Feira de Santana, Bahia, Brazil
 <sup>2</sup> Federal University of Reconcavo of Bahia (UFRB), Energy Engineering Department, Feira de Santana, Bahia, Brazil
 <sup>3</sup> Federal University of Bahia (UFBA), Electrical and Computer Engineering, Salvador, Bahia, Brazil
 <sup>4</sup> Federal University of Bahia (UFBA), Energy Efficiency Lab (LABEFEA), Salvador, Bahia, Brazil
 \*Federal University of Reconcavo of Bahia (UFRB); Feira de Santana, Bahia; tarsila@aluno.ufrb.edu.br

Abstract: The growth of Distributed Generation (DG) from renewable energy sources significantly impacts the operation of electrical power systems. To enable the efficient integration of these sources into the electrical grid, inverters play a fundamental role by converting direct current (DC) into alternating current (AC). This study aims to present a simplified design project, implemented and tested through simulations in the MATLAB Simulink environment. The goal is to make resonant control techniques and active damping through capacitor current feedback more accessible and easier to understand, as well as to evaluate and demonstrate the effectiveness of the proposed methods, enabling their practical application. The results obtained showed that the control techniques employed are essential to ensure stability and power quality in inverters with LCL filters. The methodology was presented in a clear and objective manner, facilitating understanding. The simulations highlighted the reduction of the resonance peak, the effective control of the current injected into the grid, and low THD values, confirming the feasibility of applying these techniques in renewable energy systems connected to the electrical grid. Keywords: Inverters. LCL Filter. Active Damping. Resonant Control.

#### 1. Introduction

The growth of Distributed Generation (DG) from renewable energy sources significantly affects the operation of electrical power systems. The increasing penetration of photovoltaic, wind, and other grid-connected DG technologies requires viable strategies to mitigate such impacts related to harmonic distortion and stability [1].

In this context, the efficient integration of renewable energy generation systems into the electrical grid requires the use of inverters, whose primary function is to convert direct current (DC) into alternating current (AC) with high dynamic performance and compliance with power quality standards [2]. To meet these standards, filters are employed. Among the most

commonly used types are the inductive (L) filter, applied in low-power systems and characterized by its simple design; the inductive-capacitive (LC) filter, which provides better harmonic reduction performance than the L filter; and the inductive-capacitive-inductive (LCL) filter, which offers the highest efficiency in attenuating high-frequency harmonics. The most widely used filter topology is the LCL, designed to attenuate high-frequency harmonic components generated by pulse width modulation (PWM) and to ensure the injection of current with low harmonic content.

The LCL filter can be implemented using passive or active damping techniques. In the passive approach, resistors are inserted — either in series or in parallel with the inductive and

ISSN: 2357-7592





capacitive elements — with the purpose of dissipating energy at the resonance frequencies. Although simple to implement, this technique results in additional power losses due to the Joule effect, which negatively impacts the overall efficiency of the converter [3].

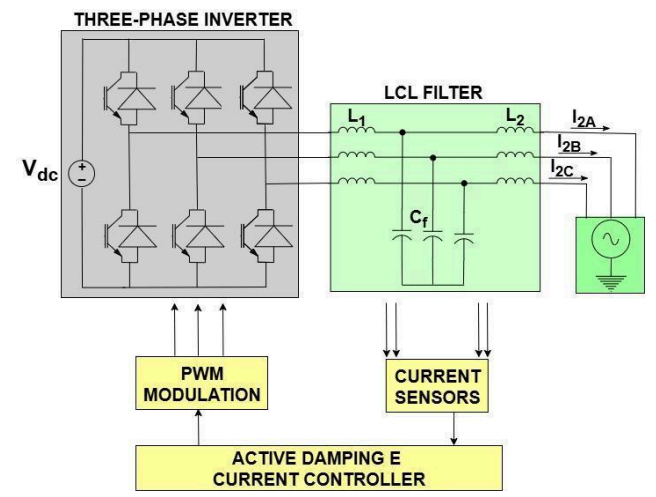
The active damping, on the other hand, incorporates control strategies capable of suppressing filter resonance without introducing resistive losses, as in the case of capacitor current feedback. This approach improves system stability and preserves energy efficiency. However, it increases the complexity of the control design due to the dynamic coupling between the damping action and the inverter current control loop, which may reduce stability margins [3].

This work presents the steady-state performance analysis of a control system applied to a grid-connected inverter equipped with an LCL filter and active damping through capacitor current feedback, combined with a resonant-type current controller [4]. A simplified design procedure proposed facilitate implementation validation and through Simulink/MATLAB simulations in the environment, making the control techniques more accessible and understandable, as well as quantitatively evaluating their effectiveness and demonstrating their feasibility for application in renewable energy systems connected to the electrical grid.

### 2. System Modeling

The design and sizing of the proposed system follow the methodological guidelines described in [4], ensuring consistency among modeling, implementation, and validation, in accordance with well-established methodologies recognized in the specialized literature, thereby reinforcing the relevance and reliability of the adopted approach. The modeled electrical circuit consists of a three-phase inverter connected to grid through power Inductor-Capacitor-Inductor (LCL) filter, associated with a resonant control system composed of active damping and a current controller. This controller is responsible for regulating the three-phase currents  $I_{2A}$ ,  $I_{2B}$ , and  $I_{2C}$  (see Figure 1).

Figure 1. Proposed Electrical System



In Figure 1, the presence of current sensors can be observed, which provide information to the digital control system that, in turn, determines the logical state of the inverter's electronic switches. It is worth noting that the renewable energy source at the inverter



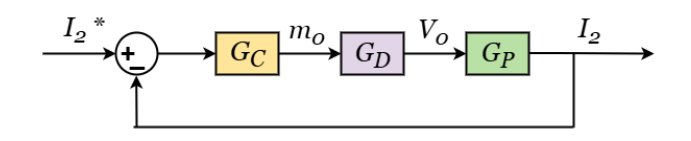


input is represented by an ideal direct voltage bus (VDC), while the grid is represented by its Thevenin equivalent. In this work, the LCL filter is used to attenuate high-frequency harmonics generated by the modulation process, ensuring that the current injected into the grid has a low total harmonic distortion (THD) as established by IEEE 519. Another important feature is that this type of filter exhibits a characteristic attenuation of 60 dB/decade, making it generally designs requiring compact suitable for components. However, the LCL filter introduces a resonance peak between the cutoff frequency and the switching frequency, requiring the use of damping techniques—in this study, active damping via capacitor current feedback—to ensure system stability and robustness.

### 2.1 Control System Stability

The stability analysis of the converter current control system begins with obtaining the transfer function of the LCL filter without damping, considering a reference current  $I_2^*$  (Figure 2). This modeling allows for the evaluation of the system dynamics and the identification of stability conditions prior to the inclusion of active damping [4].

**Figure 2.** Block Diagram of the  $I_2$  Current Control without Damping



In the block diagram, the  $G_c$  subsystem represents the resonant current controller, responsible for adjusting the error between the measured current and the reference. The  $G_{\rm p}$ subsystem models the behavior of the modulation process and its dynamic effect on the inverter switches. This block includes the delays introduced by the analog-to-digital conversion of the current. The  $G_p$  subsystem describes the plant represented by the LCL filter, considering the electrical parameters obtained from the design. This modular approach enables the frequency-domain application analysis techniques (Bode diagrams) for the evaluation of gain and phase margins, robustness, and dynamic performance, allowing fine-tuning of the control parameters to ensure stability and low THD of the current injected into the grid in accordance with power quality standards.

The  $G_C$  block is represented in continuous time by:

$$G_{C}(s) = K_{p} \left( 1 + \frac{1}{T_{r}(s^{2} + \omega_{0}^{2})} \right)$$
 (1)

where  $K_p$  is the proportional gain and  $T_r$  is the time constant, both of which need to be properly tuned. In addition,  $\omega_0$  represents the fundamental frequency of the electrical grid.

The  $G_D$  transfer function is required to represent the time delay that occurs in the inverter when controlled by PWM modulation, as this switching does not occur instantaneously.





In Equation 2,  $T_d$  can be approximated as 1.5 times the sampling period  $T_c$ .

$$G_{D}(s) = V_{dc} e^{-sT_{d}}$$
 (2)

For the  $G_p$  block, which represents the behavior of the LCL filter, the following transfer function is obtained:

$$G_p(s) = \frac{I_2(s)}{V_0(s)} = \frac{\gamma_{LC}^2}{sL_1(s^2 + \omega_r^2)}$$
 (3)

where 
$$\gamma_{LC} = \sqrt{1/(L_2 C_f)}$$
 and

 $\omega_r = \sqrt{L_1 + L_2/L_1L_2C_f}$  refers to the resonance frequency of the filter.

The internal current control loop is not limited to attenuating the gain peak associated with the resonance frequency of the LCL filter; it also plays a crucial role in expanding the system's stability regions, thereby increasing its robustness against parametric variations. From the Bode diagram analysis of the transfer function illustrated in Figure 2 — corresponding to the system without damping — it can be observed that system stability is directly related to the positioning of the filter's resonance frequency. More specifically, the system remains stable when it is within the range between  $f_c/6$  and  $f_c/2$ , with the critical frequency defined as  $f_c = 1/T_s$ , as shown in Figure 3 [5].

Figure 3 presents the Bode diagram for four different resonance frequency values, showing that  $f_1$  and  $f_2$  are located in the unstable region, while  $f_3$  and  $f_4$  fall within the stability range predicted by the analysis. This characterization not only allows the evaluation of the system's dynamic performance but also enables the definition of design criteria for the correct positioning of  $f_r$ , in order to avoid critical phase crossings that could compromise the stability margin.

Source: T. G. Oliveira et al. (2019)

An alternative to stabilize the control system with a resonance frequency lower than the critical frequency is the strategy known as active damping. In this approach, an internal loop is added to the control system with the purpose of attenuating the resonance phenomenon. The capacitor current was used as the feedback variable for active damping. The scheme, in terms of a block diagram, is presented in Figure 4. In this diagram, the transfer functions  $G_{ic}$  and  $G_{i2}$  are added, which



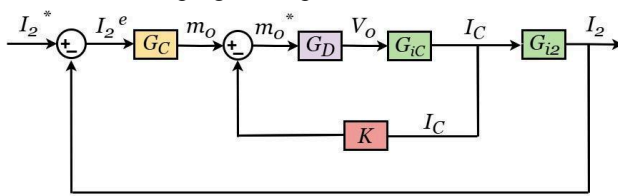


are derived from  $G_p$ . The parameter K is a damping gain to be adjusted in the control design, where:

$$G_{iC}(s) = \frac{1}{sL_1} \frac{s^2}{s^2 + \omega_{\perp}^2}$$
 (4)

$$G_{i2}(s) = \frac{\gamma_{LC}^2}{s^2} \tag{5}$$

**Figure 4.** Block Diagram of the  $I_2$  Current Control with Active Damping via Capacitor Current Feedback



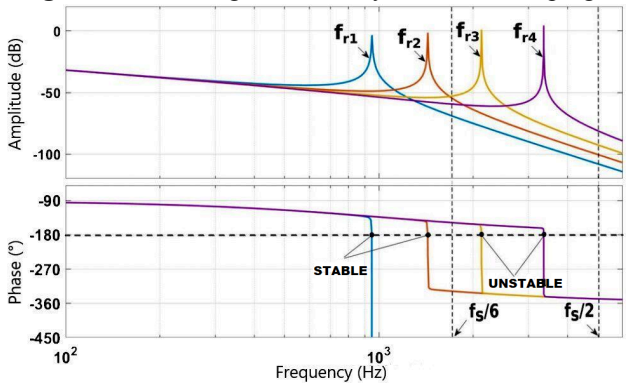
The Figure 5 again shows the Bode diagram after the application of active damping, plotted for the same four resonance frequencies as in Figure 3. It can be observed that this technique provides significant attenuation of the resonance peak magnitude, reducing the excessive gain at  $f_r$ .

With the inclusion of active damping, a swapping between the stable and unstable regions can be observed compared to the case without damping. Specifically, the frequencies  $f_{r1}$  and  $f_{r2}$ , previously located in the unstable region, now exhibit stable conditions, while  $f_{r3}$  and  $f_{r4}$ , formerly stable, become unstable. The swapping of these zones can be advantageous, as it allows the expansion of the stability region through additional strategies, such as the use of a phase-lead compensator capable of increasing

the critical frequency [6]. Thus, the results can be summarized as follows:

$$\forall f_r \in R, f_r < \frac{f_c}{6} \Rightarrow Stable System (6)$$

Figure 5. Bode Diagram of the System with Damping



Source: T. G. Oliveira et al. (2019)

Thus, the expansion of the stability region facilitates the tuning process of the resonant current controller parameters ( $K_p$  and  $T_r$ ), increasing the range of viable parameter combinations that ensure system stability.

### 3. Resonant (PR) Controller Design

As seen in [4], the design of  $K_p$ ,  $T_r$ , and K is carried out using the pole-placement technique and root locus analysis. The system's frequency response must satisfy a desired gain margin at the phase crossover frequency  $(\omega_c)$ , safely greater than 6 dB, and a phase margin between 45° and 60°  $(\phi_m)$ , to ensure controllability. Thus, it is necessary to heuristically set values of  $\omega_c$  to achieve a frequency response that meets the phase margin specification  $\phi_m$ . It is worth noting that a good starting point is to use  $\omega_c$  values close to those





given by Equation 7, which are determined from the analysis of the  $I_2$  (output) and  $I_2^{e}$  (current error) currents, as shown in Figure 4. From the value of  $\omega_C$ , the gains  $K_p$  and  $T_r$  are obtained according to Equations 8 and 9, which are also determined from the Block Diagram analysis expressed in Figure 4. Following methodology and derivations in [4], a value of K can then be selected based on the limits established by the filter parameters. However, in this work, the possible values of K were determined heuristically, taking into account the criteria for the aforementioned gain and phase margins.

$$\omega_{\mathcal{C}} = \frac{\frac{\pi}{2} - \Phi_{m}}{\frac{3Ts}{2}} \tag{7}$$

$$K_P \approx \frac{\omega_c \left(L_1 + L_2\right)}{V_{c.}}$$
 (8)

$$T_r = \frac{10}{\omega_c} \tag{9}$$

### 4. Simulation Results

In this section, the results obtained through simulations conducted in the MATLAB Simulink environment under steady-state conditions are presented. The simulations were carried out using the parameters shown in Table 1, which summarizes the design of the LCL filter and the resonant controller. To ensure effective damping of the system, it was stipulated that  $f_r < f_c/6$ , in addition to selecting a phase margin  $(\phi_m)$  between 45° and 60°.

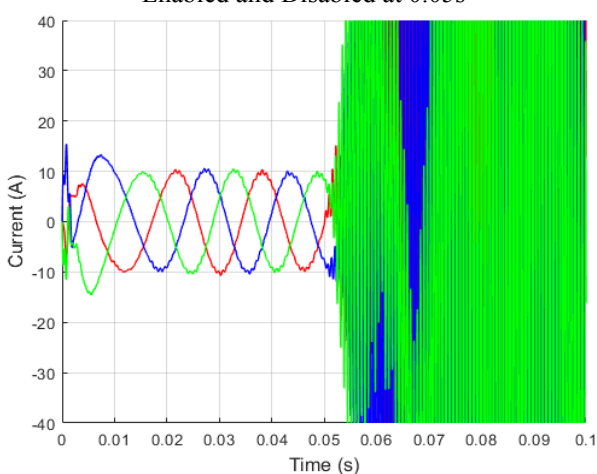
Table 1. System Parameters

| Parameter    | Value      |
|--------------|------------|
| $L_1$ (H)    | 0.00763433 |
| $L_2$ (H)    | 0.00458060 |
| $C_f$ (F)    | 0.00000393 |
| $f_c$ (Hz)   | 10000      |
| $f_r$ (Hz)   | 1500.9379  |
| $T_r$ (s)    | 0.0032     |
| $K_p$        | 38.3476    |
| $V_{dc}$ (V) | 325        |

## 4.1. Output Current Behavior of the LCL Filter

The Figure 6 shows the current waveforms of the three phases of the system over time. It can be observed that, up to 0.05s, with active damping enabled, the waveforms are sinusoidal, symmetrical, stable, and maintain an amplitude around 10A, indicating that the controller was able to satisfactorily track the reference. However, from 0.05scurrent onwards, with the deactivation of active damping, there is an abrupt and significant increase in the current amplitudes, exceeding 30A, resulting in a progressively oscillatory behavior and consequent system instability.

**Figure 6.** Simulation of the System with Damping Enabled and Disabled at 0.05s



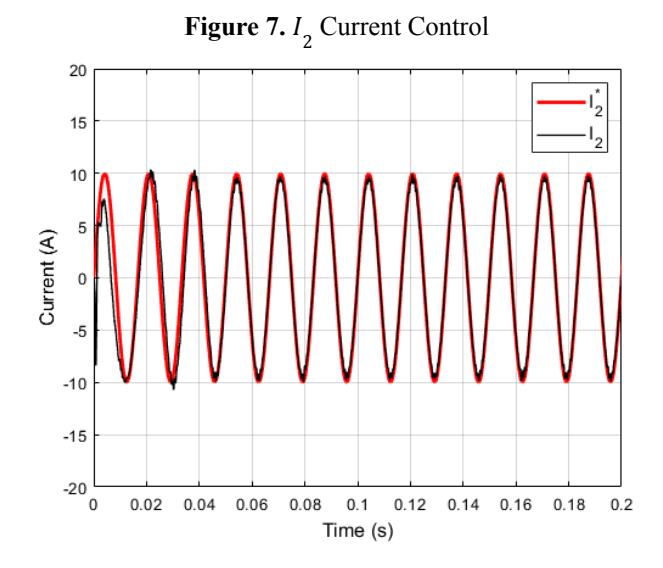




The impact of deactivating active damping on the system can be clearly observed, as evidenced by the uncontrolled behavior of the currents. The removal of the damping loop causes the amplification of the LCL filter's resonance peak, which then operates within an unstable region, resulting in increasing oscillations and loss of system stability. This phenomenon highlights the critical importance of active damping strategies, such as capacitor current feedback, which shift the resonance pole to a stable region of the complex plane, expanding the system's stability zone. In this way, robust and stable operation of the inverter is ensured, even in the presence of parametric variations and adverse operating conditions.

### 4.2. Resonant Control (PR) Performance

In Figure 7, a comparison is made between the reference current  $({\cal I}_2^{\phantom{2}})$  and the measured output current  $(I_2)$ , controlled by a resonant (PR) controller. The controller demonstrates a high tracking capability, with an almost negligible tracking error, resulting in an almost perfect overlap between the measured and the reference. Both exhibit current sinusoidal characteristics with low harmonic distortion, highlighting the effectiveness of the PR controller in ensuring dynamic accuracy and the quality of the current injected into the system.



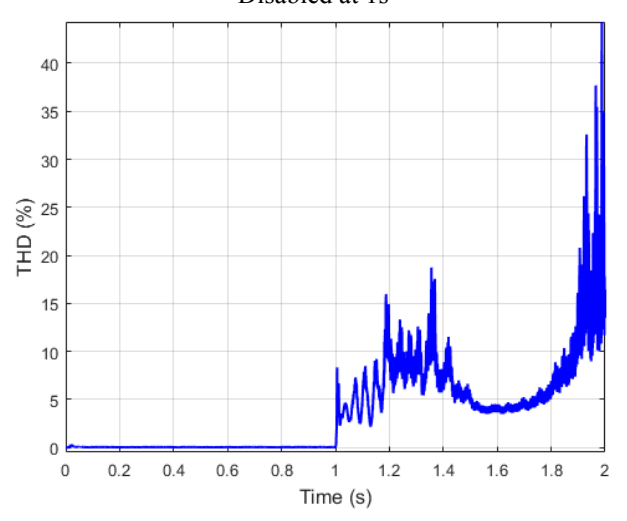
# 4.3. Total Harmonic Distortion (THD) Analysis

The Figure 8 presents the THD results measured in the output current of the LCL filter, i.e., the current directly injected into the distribution grid. From the beginning of the simulation up to 1 s, active damping is in operation, keeping the THD below 5% and fully complying with the limits established by IEEE 519 (5%) and ANEEL PRODIST - Module 8 (10%) [2], [7], which demonstrates high power quality. After 1 s, due to the deactivation of damping, system instability occurs, causing the THD to rise above 40%. These results confirm that active damping is not only fundamental for dynamic stability but also essential to ensure that the injected current remains within the harmonic distortion limits established by power quality standards.





**Figure 8.** System THD with Control Enabled and Disabled at 1s



### 5. Conclusion

This paper presented a study on the simplified design of a resonant (PR) controller combined with an active damping scheme implemented via capacitor current feedback, following the procedures described in the established literature, as detailed in [4]. The results demonstrate that the use of active damping through capacitor current feedback, together with the PR controller, is essential to ensure dynamic stability and power quality in grid-connected inverters with LCL filters.

methodology The adopted for the development of these control techniques was described in a clear and structured manner, facilitating their understanding and practical application. The simulations demonstrated effective attenuation of the resonance peak, precise regulation of the current injected into the grid, and maintenance of low THD levels, meeting the regulatory requirements. These characteristics make the proposed solution technically feasible for applications in grid-connected renewable generation systems.

For future works, it is recommended to extend the analyses to the transient regime in order to evaluate the dynamic behavior of the system under different operating conditions. In addition, the application of other design and sizing methodologies, also recognized in the literature, could be considered to complement or enhance the results obtained in this study.

### References

- [1] Iweh, C.D.; Gyamfi, S.; Tanyi, E.; Effah-Donyina, E. Distributed Generation and Renewable Energy Integration into the Grid: Prerequisites, Push Factors, Practical Options, Issues and Merits. Energies 2021.
- [2] "IEEE Standard for Harmonic Control in Electric Power Systems," in IEEE Std 519-2022 (Revision of IEEE Std 519-2014), vol., no., pp.1-31, 5 Aug. 2022, doi: 10.1109/IEEESTD.2022.9848440.
- [3] J. B. C. Ribeiro, Avaliação do Filtro LCL Interligado à Rede Elétrica Utilizando Técnicas de Amortecimento Passivo e Ativo. 2018. 92 f. TCC (Graduação) - Curso de Engenharia Elétrica, Universidade Federal de Mato Grosso do Sul, Campo Grande, 2018.
- [4] S. G. Parker, B. P. McGrath, and D. G. Holmes, "Regions of active damping control for lcl filters," IEEE Trans. Ind. Appl., vol. 50, no. 1, pp. 424–432, Jan./Feb. 2014.
- [5] Z.Xin,X.Wang,P.C.Loh, andF.Blaabjerg, "Grid-current-feedback control for lcl-filteredgrid converterswith enhanced stability," IEEE TransactionsonPowerElectronics,vol.32,no.4,pp.3216 –3228,Apr. 2017.
- [6] Z. Xin, X. Wang, P. C. Loh, and F. Blaabjerg, "Grid-current-feedback control for lcl-filtered grid converters with enhanced stability," IEEE Trans Power Eletron., 2017.
- [7] ANEEL, *Procedimentos de Distribuição PRODIST*, Módulo 8: Qualidade da Energia Elétrica.
- [8] T. G. Oliveira; U. S. Araújo; J. R. Pinheiro; A. P. N. Tahim; F. F. Costa. "Avaliação de estabilidade e projeto de controladores para inversores LCL conectados à rede elétrica." Seminar on Power Electronics and Control (SEPOC), Natal, 2019.